

# Electrochemical Reduction of G3-Factor Endoperoxide and Its Methyl Ether: Evidence for a Competition between Concerted and Stepwise Dissociative Electron Transfer

Fadia Najjar,<sup>[a]</sup> Christiane André-Barrès,<sup>\*[a]</sup> Michel Baltas,<sup>[a]</sup> Corinne Lacaze-Dufaure,<sup>[b]</sup> David C. Magri,<sup>[c]</sup> Mark S. Workentin,<sup>[c]</sup> and Théodore Tzédakis<sup>[d]</sup>

**Abstract:** The reduction of the bicyclic G-factor endoperoxides G3 and G3Me was studied in *N,N*-dimethylformamide using cyclic voltammetry and convolution analysis. Electron transfer leads to irreversible cleavage of the O–O bond. Detailed analysis of the voltammetry curves reveals a non-linear dependence

on the transfer coefficient indicating a mechanistic transition from a stepwise mechanism to one with more concerted

character with increasing potential. By using quantum calculations to estimate the O–O bond dissociation energies, the experimental data was used to evaluate the standard reduction potentials and other pertinent thermochemical information.

**Keywords:** electrochemistry · electron transfer · endoperoxide · radical ions

## Introduction

The first step in the reduction mechanism of antimalarial endoperoxides, such as artemisinin, is believed to be an electron transfer (ET) from heme-iron<sup>[1–3]</sup> or free iron<sup>[4a,b]</sup> resulting in the cleavage of the O–O bond. The generated alkoxy radicals are believed to rearrange to carbon-centered radicals, and alkylate heme and proteins.<sup>[1c,2b]</sup>

A goal of one of our research groups is the synthesis of bicyclic endoperoxides belonging to the G-factor series. These natural products, extracted from the leaves of *Euca-*

*lyptus grandis* and other *myrtaceae*, are known phytohormones and growth regulators.<sup>[5]</sup> We have previously reported the synthesis, antimalarial properties, and redox behavior of some of these G-factors derivatives.<sup>[6,7]</sup> An intriguing finding was that the in vitro antimalarial activity of G3-factor (IC<sub>50</sub> = 36 μM on *Plasmodium falciparum* Nigerian strains sensitive to chloroquine) was found to be 100-fold less active than its methyl ether (IC<sub>50</sub> = 0.28 μM).<sup>[7b]</sup> As a result, we were curious about the significance of substituent effects on antimalarial potency. Thus, we began a study on the dissociative ET reduction of the O–O bond of G3 and G3Me in order to gain further mechanistic insight.

The O–O bond reduction of model endoperoxides, as well as artemisinin, has been shown to occur by a concerted dissociative ET mechanism.<sup>[8–10]</sup> In the concerted mechanism, the electron is accepted into the σ\* orbital, largely associated with the O–O bond, resulting in simultaneous (on the order of a bond vibration) cleavage to generate a spatially separated alkoxy radical and an alkoxide, 'ORRO', known as a distonic radical anion (Scheme 1). With the model endoperoxides, ascaridole and dihydroascaridole, the distonic radical anion is reduced at the electrode resulting in the quantitative formation of the *cis*-diols by a mechanism requiring the overall consumption of two electrons per molecule.<sup>[10]</sup> There is also the possibility of a stepwise dissociative mechanism, for example, when there is an energetically accessible π\* orbital within the molecule. In the stepwise mechanism, the initial ET results in the formation of an in-

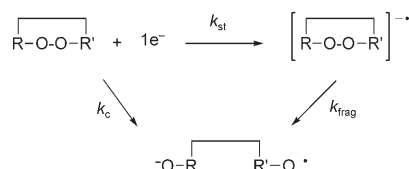
[a] Dr. F. Najjar, Dr. C. André-Barrès, Dr. M. Baltas  
Laboratoire de Synthèse et Physicochimie de Molécules d'Intérêt Biologique, CNRS UMR 5068 Université Paul Sabatier, 118 route de Narbonne, 31062 Toulouse (France)  
Fax: (+33) 561-558-245  
E-mail: candre@chimie.ups-tlse.fr

[b] Dr. C. Lacaze-Dufaure  
Centre Interuniversitaire de Recherche et d'Ingénierie des Matériaux, CNRS UMR 5085, ENSIACET, 118 route de Narbonne 31077 Toulouse Cedex 4 (France)

[c] Dr. D. C. Magri, Prof Dr. M. S. Workentin  
Department of Chemistry, the University of Western Ontario, London, ON N6A 5B7 (Canada)

[d] Prof. Dr. T. Tzédakis  
Laboratoire de Génie Chimique, CNRS UMR 5503 Université Paul-Sabatier, 118 route de Narbonne, 31062 Toulouse (France)

Supporting information for this article is available on the WWW under <http://www.chemeurj.org/> or from the author.



Scheme 1. Representation of a possible mechanism for electrochemical reduction of the -O-O- bound.

intermediate radical anion followed by cleavage of the O-O bond ( $k_{\text{frag}}$ ) in a second step. Evidence for a stepwise dissociative ET, and even the transition from a concerted to a stepwise ET (Scheme 1), has been observed within series of perbenzoates and peresters.<sup>[11]</sup> The overall competition between the two mechanisms is dependent on various intrinsic properties of the reactive compound and the reduction conditions.<sup>[11,12]</sup>

In this study, the G-factor analogous endoperoxides G3 and G3Me are investigated using cyclic voltammetry followed by convolution analysis of the data to gain insight into the reduction mechanism of the O-O bond. We report examples of endoperoxides that undergo a competitive concerted versus stepwise dissociative ET. Analysis of the experimental data provides estimates of many thermochemical parameters, notably the standard reduction potentials, which are necessary for estimating the energetics for ET from potential biological donors (Figure 1).

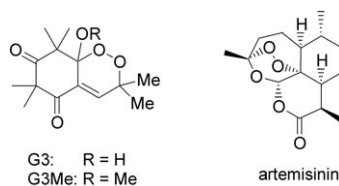


Figure 1. G3-factor, methylated G3-factor and artemisinin.

## Experimental Section

Electrochemical experiments were performed with a Perkin-Elmer-Princeton Applied Research (PAR 263A) potentiostat/galvanostat in anhydrous *N,N*-dimethylformamide (DMF) at 25 °C under an argon atmosphere in the presence of 0.10 M tetraethylammonium perchlorate (TEAP). A three electrode set-up was used as previously described.<sup>[10]</sup> The working electrode was either a 1 or 3 mm diameter glassy carbon rod (Tokai, GC-20). Before each experiment, the working electrode was carefully polished on an abrasive felt using a diamond past, rinsed and sonicated in 2-propanol for 10 min and finally dried with a stream of cool air. The electrode was activated by cycling several times between 0 to -2.8 V at a scan rate of 0.2 V s<sup>-1</sup>. A 1 cm<sup>2</sup> platinum blade was used as the auxiliary electrode. The reference electrode was a silver wire immersed in a glass sintered tube containing a 0.1 M solution of TEAP in DMF. It was calibrated after each experiment against the ferrocene/ferricenium couple (0.475 V vs SCE). A feedback correction was applied to minimize the ohmic drop between the working and reference electrodes. Coulometric measurements were performed using a 12 mm glassy carbon an EDI101 rotating disk electrode from Radiometer Analytical.

The syntheses of G3 and G3Me endoperoxides have been previously reported.<sup>[6,7a]</sup>

## Results and Discussion

The electrochemical reduction of G3 and G3Me was studied by cyclic voltammetry using a glassy carbon electrode in anhydrous *N,N*-dimethylformamide (DMF) containing 0.10 M anhydrous tetraethylammonium perchlorate (TEAP). The voltammetry of each endoperoxide, as shown in Figure 2, is initially characterized by a cathodic peak located at -1.60 and -1.50 V vs SCE for G3 and G3Me, respectively. These peaks are attributed to the reduction of the O-O bond. On the backward scan, no signal corresponding to these peaks is observed, indicating the irreversible reduction of endoperoxides G3 and G3Me. The cathodic curve of G3 indicates two additional signals at -2.20 and -2.40 V, and associated anodic couples at -2.03 and -2.23 V. These signals suggest the formation of reversible redox products resulting from O-O bond reduction; the magnitude of these peaks is lower than the first. In contrast, G3Me exhibits much simpler voltammograms reminiscent of previously studied endoperoxides.<sup>[9,10]</sup> As the objective of the current study was to evaluate thermochemical information on the O-O bond reduction, we have focused our analysis on the first cathodic wave.

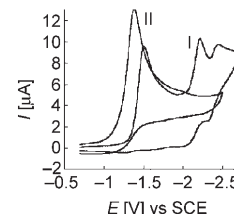


Figure 2. Voltammetric curves plotted on glassy carbon disk shaped, with G3 (I) and G3Me (II) endoperoxides at 2 mm in DMF and in presence of TBAP;  $r=0.2 \text{ V s}^{-1}$ .

Upon increasing the scan rate,  $\nu$ , from 0.1 to 40 V s<sup>-1</sup> (Figure 3(Ia), (IIa)); the analysis of Figures 2 and 3 is shown in Figure 5), the peak potential of the first signal  $E_p$  is found to shift negatively by only 41 mV per log decade. The conventional voltammetry analysis of the reduction peak reveals other anomalous features. The peak width  $\Delta E_{p/2}$ , the difference between  $E_{p/2}$  and  $E_p$  follows a parabolic dependence against the scan rate; it is found to decrease from 0.1 V s<sup>-1</sup> until about 1 V s<sup>-1</sup> and then increases at higher scan rates. The non-linear dependence is most striking with G3Me where the  $\Delta E_{p/2}$  varies from 98 to 76 to 94 mV at 0.1, 1.0 and 10 V s<sup>-1</sup>, respectively. As a consequence the apparent transfer coefficient from the  $\Delta E_{p/2}$  is found to be 0.49, 0.63, and 0.51. The significance is that not only is the transfer coefficient potential dependent, but also varies non-linearly. These findings are in contrast to studies on other bicyclic endoperoxides, which are shown to undergo a concerted dissociative mechanism.<sup>[9,10,13]</sup> Indeed, the transfer coefficient ( $\alpha$ ) represents the dependence of the intrinsic barrier against the free energy; it is correlated to the potential and the electron transfer constant  $k_{\text{ET}}$  by the relation (1):

$$\alpha = \frac{\partial \Delta G^\ddagger}{\partial \Delta G_0} = 0.5 + \frac{F(E-E^0)}{8\Delta G_0^\ddagger} = \frac{-RT}{F} \frac{d \ln k_{\text{ET}}}{dE} \quad (1)$$

For reactions following a concerted mechanism, the peak potential is overvalued in comparison to the standard poten-

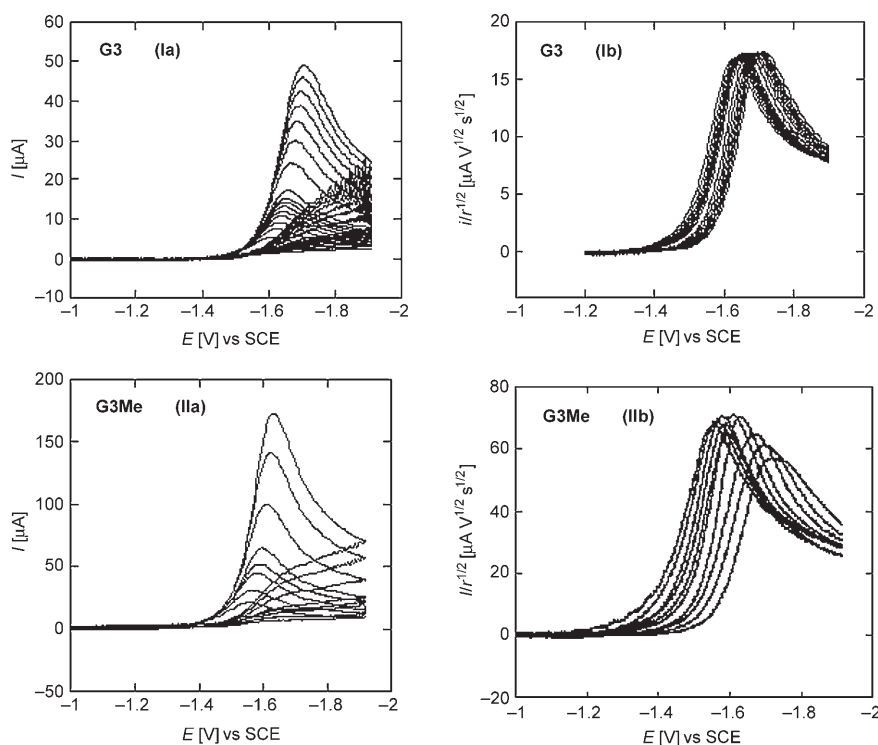


Figure 3. Voltammetric curves plotted on glassy carbon disk shaped cathode, with G3 (Ia) and G3Me (IIa) endoperoxides at 2 mm into DMF and in presence of TEAP;  $r$  is in the range 0.1 to 40  $\text{Vs}^{-1}$ . Residual current was removed and the potential is calibrated against the comparison electrode previously described. Curves (Ib) and (IIb) correspond to the normalized current against the potential scan rate.

tial because it takes account of the bond dissociation energy; consequently results from Equation (1) led to values lower than 0.3. On the other hand, for a stepwise mechanism, the magnitude of the peak potential is similar to the standard potential and values of  $\alpha$  are equal (or slightly higher) to 0.5. The present results are consistent with a stepwise dissociative reductive mechanism.<sup>[12]</sup> The voltammetry data are summarized in Table 1.

The curves (Ib) and (IIb) on the Figure 3 show that the normalized current ( $i/r^{1/2}$ ) decreases when the potential scan rate is increased; the variation in the case of G3Me is about  $10 \mu\text{AV}^{-0.5}\text{s}^{0.5}$  for  $r$  in the range 0.1 to 40  $\text{Vs}^{-1}$ . The modification is less obvious for G3 ( $\Delta i/r^{1/2} \sim 1 \mu\text{AV}^{-0.5}\text{s}^{0.5}$  for  $0.1 \leq r \leq 40 \text{Vs}^{-1}$ ). This evolution confirms that there is a chemical reaction taking place during the electrode process.

Constant potential electrolyses were performed at a glassy carbon rotating disk electrode. The current intensity of the voltammetry peak was observed to decrease as a function of the charge  $q$  consumed according to Faraday's law  $q = nFm$  where  $n$  is the number of electron equivalents,  $F$  is Faraday's constant, and  $m$  is the number of mols of endoperoxide consumed. The results from the coulometry experiments are included in Table 1. Electrolyses performed at  $-1.4 \text{V}$  results in the exchange of  $1 \text{Fmol}^{-1}$ , or 1 electron equivalent of charge per molecule. These results are consistent with previous measurements using thin-layer electrochemistry.<sup>[7a]</sup> The exchange of only one electron suggests that the distonic radical anion generated by cleavage of the O–O bond under-

goes a chemical reaction competing with a second ET from the electrode.<sup>[13]</sup> For G3, even in the presence of a weak non-nucleophilic acid such as acetanilide, the exchanged number of electrons is still  $1 \text{Fmol}^{-1}$ . In contrast, addition of acetanilide to a solution containing G3Me results in the consumption of nearly 2 electrons per mol. This is in agreement with the increase of the current when the reduction of the G3Me endoperoxide takes place in presence of acetanilide (voltammetric measurements not reported here). The influence of acetanilide on the reduction of endoperoxides G3 and G3Me and the electron stoichiometry is different from that observed for other endoperoxides and is likely the result of the reactivity of the generated distonic radical ions in the present case. As it was observed during  $\text{Fe}^{\text{II}}$ -in-

Table 1. Voltammetry data for reduction of G3 and G3Me in a solution of 0.10 M TEAP/DMF at 25 °C measured at a 1 mm glassy carbon electrode.

	Scan rate [ $\text{Vs}^{-1}$ ]	G3	G3Me
$E_p$ [V] vs SCE <sup>[a]</sup>	0.1	-1.60	-1.50
	1.0	-1.65	-1.60
	10	-1.70	-1.67
$E_{p/2} - E_p$ [mV] vs SCE	0.1	82	98
	1.0	75	76
	10	80	94
$\alpha = 1.857RT/F(E_{p/2} - E_p)$	0.1	0.58	0.49
	1.0	0.64	0.63
	10	0.57	0.51
$(dE_p/d\log v)$ [mV] <sup>[b]</sup>		48	41
$\alpha = 1.15RT/F[dE_p/d(\log v)]$		0.61	0.72
$n$ (no acid) <sup>[c]</sup>		0.92	0.95
$n$ (acid) <sup>[c,d]</sup>		1.07	1.86

[a] Potentials are referenced versus ferrocene: 0.475 V vs SCE in 0.1 M TEAP/DMF. [b]  $dE_p/d(\log v)$  based on scan rates between 0.1 and 10  $\text{Vs}^{-1}$ . [c] The number of electron equivalents consumed during electrolysis. [d] In the presence of acetanilide [ $pK_a(\text{DMF}) = 22.3$ ].

duced degradation<sup>[7e]</sup> the O-centered radical quickly rearranges in C-centered which is stabilized by the *gem*-dimethyl and the withdrawing effect of the carbonyl function. Then this C-centered radical will differently evolve in the presence or absence of acetanilide. These electrolyses give com-

plex mixtures of products and work is in progress to analyze them in each case.

Convolution analysis<sup>[14]</sup> was used to more accurately examine the nature of the electrode reduction of G3 and G3Me. The analysis was performed on experiments done in the presence of acetanilide to ensure constant electron consumption on the time scale of the experiments. Thus, it was assumed that two electrons are exchanged for G3Me and only one in the case of G3. Background subtracted voltammograms of the first irreversible wave were obtained between the scan rates of 0.1 and 50 V s<sup>-1</sup>. For an irreversible process in the electrode the data was converted to a curve having a sigmoidal-shaped using the following logarithmic Equation (2) where the ( $I_{\text{lim}}$ ) is the convoluted limiting current,  $i(t)$  the real current and  $k_{\text{ET}}^{[15]}$  is the heterogeneous rate constant.

$$\ln k_{\text{ET}} = \ln D^{0.5} - \ln \frac{[I_{\text{lim}} - I(t)]}{i(t)} \quad (2)$$

At the plateau of the convoluted curves (Figure 4) the electrode reaction is diffusion controlled such that the limiting current is expressed by  $I_{\text{lim}} = nFA D_{\text{Ox}}^{1/2} C^*$  where  $n$  is the overall electron consumption,  $A$  is the electrode area,  $D$  is the diffusion coefficient, and  $C^*$  is the concentration of substrate. The convoluted limiting current was found to be consistent and independent of the potential with an error less than 5%, which allowed for the evaluation the diffusion coefficients of  $6.9 \times 10^{-6}$  and  $6.4 \times 10^{-6}$  cm<sup>2</sup> s<sup>-1</sup> for G3 and G3Me, respectively. Derivatization of the  $\ln k_{\text{het}}$  allows the evaluation of the apparent transfer coefficient uncorrected for the double layer according to Equation (1).

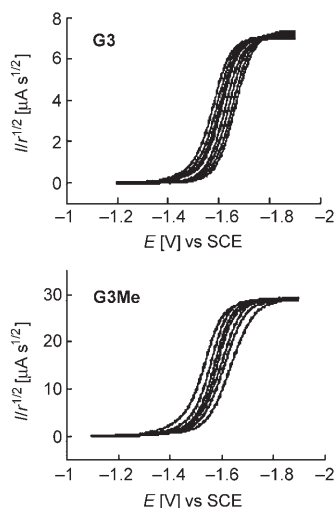


Figure 4. Convoluted curves for various potential scan rates ( $r$ ) in the range 0.1 to 40 V s<sup>-1</sup> for G3 and G3Me endoperoxides.

The data were derivatized in steps of 15 to 21 mV yielding the parabolic-shaped curves, for both endoperoxides, as depicted in Figure 6. In the case of a purely concerted or step-

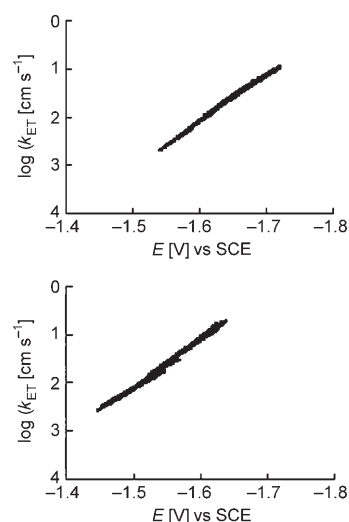


Figure 5.  $\log k_{\text{ET}}$  as a function of the potential for G3 and G3Me; (analysis of curves of Figures 2 and 3).

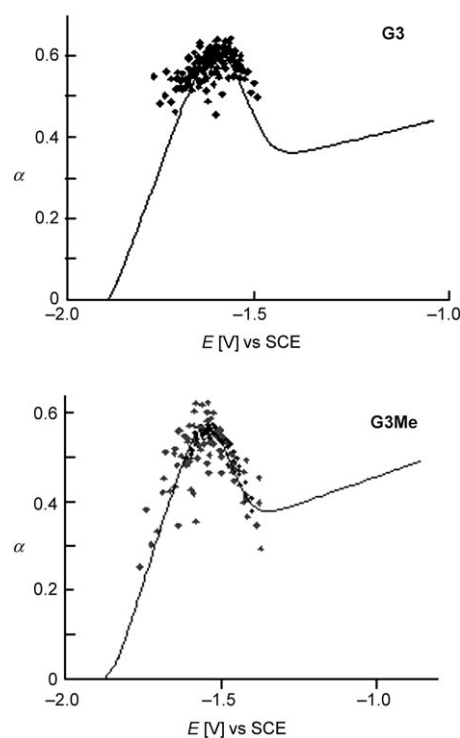


Figure 6. Dependence of the electron transfer coefficient ( $\alpha$ ) versus the potential; points: experimental results (two sets of values for G3Me), continuous line: theoretical evolution.

wise mechanism, the transfer coefficient  $\alpha$  varies linearly with the applied potential. The standard reduction potential can be obtained by a linear extrapolation to  $\alpha = 0.5$ . Furthermore, the heterogeneous rate constant  $k_{\text{ET}}$  for ET is expressed by Equations (3), (4) and (5). The activation energy  $\Delta G^\ddagger$  is related to the free energy for ET  $\Delta G^0$  by the Marcus quadratic Equation (3):

$$\Delta G^\ddagger = \Delta G_0^\ddagger \left( 1 + \frac{\Delta G_0}{4\Delta G_0^\ddagger} \right)^2 \quad (3)$$

According to Savéant's dissociative ET theory, the intrinsic barrier,  $\Delta G_0^\ddagger$ , is a function of the bond dissociation energy (BDE) of the fragmenting bond and the reorganization energy  $\lambda$  (4):

$$\Delta G_0^\ddagger = \frac{\lambda + \text{BDE}}{4} \quad (4)$$

In the case of a stepwise mechanism, there is no contribution from the BDE, so that Equation (4) is simplified to  $\Delta G_0^\ddagger = \lambda/4$ . Finally,  $k_{\text{ET}}$  is related to  $\Delta G^\ddagger$  by an Eyring-type Equation (5):

$$k_{\text{ET}} = Z \exp \left[ -\frac{\Delta G^\ddagger}{RT} \right] \quad (5)$$

where  $Z$  is the Arrhenius pre-exponential factor including the electronic transmission coefficient  $\kappa$ . In most cases, ET is adiabatic with  $\kappa$  set arbitrarily equal to 1. Most noteworthy, is that previous studies by Workentin, Maran and co-workers have revealed that ET to peroxides and endoperoxides is non-adiabatic with  $\kappa < 1$ .<sup>[16]</sup> The transfer coefficient ( $\alpha$ ) represents the dependence of the intrinsic barrier against the free energy; it is correlated to the potential and the electron transfer constant  $k_{\text{ET}}$  by the Equation (1).

In the case both concerted and stepwise dissociative ET occurs at the same potential, the observed  $k_{\text{ET}}$  is the sum of the individual rate constants  $k_{\text{c}}$  and  $k_{\text{st}}$  as expressed in Equation (6):

$$k_{\text{ET}} = k_{\text{c}} + k_{\text{st}} = Z_{\text{c}} \exp \left[ -\frac{\Delta G_{0\text{c}}^\ddagger}{RT} \left( 1 + \frac{\Delta G_{0\text{c}}}{4\Delta G_{0\text{c}}^\ddagger} \right)^2 \right] + Z_{\text{st}} \exp \left[ -\frac{\Delta G_{0\text{st}}^\ddagger}{RT} \left( 1 + \frac{\Delta G_{0\text{st}}}{4\Delta G_{0\text{st}}^\ddagger} \right)^2 \right] \quad (6)$$

In order to obtain meaningful information, as thoroughly described by Maran,<sup>[11]</sup> there are three parameters to consider: i) the difference between the two standard potentials,  $\varepsilon = E_{\text{c}}^0 - E_{\text{st}}^0$  ii) the ratio between the two preexponential factors,  $z = Z_{\text{st}}/Z_{\text{c}}$  and iii) the ratio between the two intrinsic barriers  $\beta = \Delta G_{0\text{c}}^\ddagger/\Delta G_{0\text{st}}^\ddagger$ . The fitting of the theoretical equations was achieved on the basis of optimal values of  $\varepsilon$ ,  $z$  and  $\beta$  chosen in a physical realistic range for considered molecules and taking into account the following criteria and methods of calculations.

The BDE were calculated from spin-polarized density functional calculations at the B3LYP/6-31G\* level of theory. For each endoperoxide, different initial geometries were considered leading to several stationary points after the ge-

ometry optimization process. These stationary points were characterized as minima by the frequencies analysis. Finally the most stable conformers corresponding to the lowest energy were retained.<sup>[17]</sup> A zero-point energy (ZPE) correction was included in the calculation. The BDE of the O–O bond was obtained from the difference between the ZPE corrected total energy of the most stable form for each molecule in its singlet and triplet state. The spin densities analysis confirmed the presence of an unpaired electron on each oxygen atom for the triplet state (biradical). Results are  $\text{BDE}_{\text{G3}} = 33.8 \text{ kcal mol}^{-1}$  and  $\text{BDE}_{\text{G3Me}} = 31.4 \text{ kcal mol}^{-1}$ . Using the same approach, the BDE for artemisinin was estimated to be  $31.2 \text{ kcal mol}^{-1}$ .<sup>[18]</sup>

The theoretical fits of the transfer coefficient  $\alpha$  are shown as a solid line (Figure 6) by adjustment of the various parameters. The evaluated parameters are summarized in Table 2. Both endoperoxides exhibit the same standard reduction potentials, within error, for both the stepwise and

Table 2. Thermodynamic data for the heterogeneous reduction of endoperoxides G3 and G3Me.

Endoperoxide	$Z_{\text{st}}/Z_{\text{c}}$	$\lambda_{\text{c}}$ [kcal mol <sup>-1</sup> ]	$\lambda_{\text{st}}$ [kcal mol <sup>-1</sup> ]	$E_{\text{c}}^0$ [V]	$E_{\text{st}}^0$ [V]	BDE [kcal mol <sup>-1</sup> ]	$\log k_{\text{ET}}$ [cm s <sup>-1</sup> ]
G3	50	15.9	3.9	-0.82	-1.70	33.8	-1.0
G3Me	50	15.5	4.4	-0.84	-1.64	31.4	-1.1

concerted mechanisms, thus demonstrating the weak dependence of the methyl group on the heterogeneous reduction. The thermodynamic standard potentials for the stepwise versus the concerted mechanisms are quite striking with determined values of -1.7 and -0.8 V, respectively. The difference in the free energy is offset by large differences in the intrinsic barriers and the magnitude of the pre-exponential factors. In the concerted mechanism, the intrinsic barrier includes the BDE so  $\Delta G_{0\text{c}}^\ddagger > \Delta G_{0\text{st}}^\ddagger$ . The evaluated values are  $\Delta G_{0\text{c}}^\ddagger = 16 \text{ kcal mol}^{-1}$  and  $\Delta G_{0\text{st}}^\ddagger = 4 \text{ kcal mol}^{-1}$ . This is expected considering that in the concerted case fragmentation of the O–O bond occurs simultaneously with ET whereas in the stepwise case the only barrier is the reorganization energy. Furthermore, the stepwise mechanism is adiabatic, whereas the concerted mechanism is known to be non-adiabatic  $Z_{\text{st}} > Z_{\text{c}}$ , which also contributes to lowering  $k_{\text{ET}}$  in the concerted case. An interesting outcome of this study is that the standard reduction potential for the concerted dissociative reduction is identical to that for artemisinin.<sup>[9a]</sup> Therefore, based on thermodynamic arguments, the feasibility for ET reduction of G3 endoperoxides from biological donors, such as heme, is expected to occur.

The  $k_{\text{ET}}^0$  was evaluated from the observed heterogeneous data with knowledge of the standard reduction potentials to be relatively fast with values of  $\sim 0.1 \text{ cm s}^{-1}$ . This is consistent with heterogeneous reduction of the conjugate ketone and a stepwise mechanism. The  $k_{\text{ET}}^0$  for concerted dissociative ET of O–O bonds are typically over three orders of magnitude lower.<sup>[13]</sup>

## Conclusion

The heterogeneous reduction of the G-factor endoperoxides G3 and G3Me demonstrates a non-linear dependence on the applied potential. We propose that this behavior results from a competition between a stepwise and concerted dissociative ET mechanism. This is the first time a competition between these two mechanisms has been observed in the case of endoperoxides. From the application of dissociative ET theory, a number of thermochemical parameters were determined notably the standard reduction potentials, the intrinsic barriers, and the pre-exponential factors. As the significant difference in biological activity between G3 and G3Me cannot be readily explained by the subtle differences in the evaluated kinetic and thermochemical data, other factors such as pharmacological or chemical reactivity of the C-centred radicals<sup>[7e]</sup> through different mechanistic pathways are to be considered.

## Acknowledgements

CNRS is acknowledged for financial support, CALMIP and CICT for providing computer time on the supercomputer Magellan. This work was also supported by "Ministère de la Recherche" through the project ACI 2000 "Colocalu" and NSERC of Canada.

- [1] a) O. Provot, B. Camuzat-Denis, M. Hamzaoui, H. Moskowitz, J. Mayrargue, A. Robert, J. Cazelles, B. Meunier, F. Zouhiri, D. Desmaële, J. d'Angelo, J. Mahuteau, F. Gay, L. Cicéron, *Eur. J. Chem.* **1999**, 1935–1938; b) A. Robert, J. Cazelles, B. Meunier, *Angew. Chem.* **2001**, *113*, 2008–2011; *Angew. Chem. Int. Ed.* **2001**, *40*, 1954–1957; c) A. Robert, F. Benoit-Vical, B. Meunier, *Coord. Chem. Rev.* **2005**, *249*, 1927–1936.
- [2] a) S. R. Meshnick, T. E. Taylor, S. Kamchonwongpaisan, *Microbiol. Rev.* **1996**, *60*, 301–315; b) S. R. Meshnick, *Int. J. Parasitol.* **2002**, *32*, 1655–1660.
- [3] P. M. O'Neill, G. H. Posner, *J. Med. Chem.* **2004**, *47*, 2945–2964.
- [4] a) U. Eckstein-Ludwig, R. J. Webb, I. D. A. van Goethem, J. M. East, A. G. Lee, M. Kimura, P. M. O'Neill, P. G. Bray, S. A. Ward, S. Krishna, *Nature* **2003**, *424*, 957–961; b) M. G. B. Drew, J. Metcalfe, F. M. D. Ismail, *J. Mol. Struct.* **2005**, *756*, 87–95.
- [5] E. Ghisalberti, *Phytochemistry* **1996**, *41*, 7–22, and references therein.
- [6] M. Gavrilan, C. André-Barrès, M. Baltas, T. Tzedakis, L. Gorrichon, *Tetrahedron Lett.* **2001**, *42*, 2465–2468.
- [7] a) F. Najjar, M. Baltas, L. Gorrichon, Y. Moreno, T. Tzedakis, H. Vial, C. André-Barrès, *Eur. J. Org. Chem.* **2003**, *17*, 3335–3343; b) F. Najjar, L. Gorrichon, M. Baltas, H. Vial, T. Tzedakis, C. André-Barrès, *Bioorg. Med. Chem. Lett.* **2004**, *14*, 1433–1436; c) F. Najjar, F. Fréville, F. Desmoulin, L. Gorrichon, M. Baltas, H. Vial, T. Tzedakis, C. André-Barrès, *Tetrahedron Lett.* **2004**, *45*, 6919–6922; d) F. Najjar, L. Gorrichon, M. Baltas, C. André-Barrès, H. Vial, *Org. Biomol. Chem.* **2005**, *3*, 1612–1614; e) C. André-Barrès, F. Najjar, A.-L. Bottalla, S. Massou, C. Zedde, M. Baltas, L. Gorrichon, *J. Org. Chem.* **2005**, *70*, 6921–6924.
- [8] F. Maran, D. D. M. Wayner, M. S. Workentin, *Adv. Phys. Org. Chem.* **2001**, *36*, 85–166.
- [9] a) R. L. Donkers, M. S. Workentin, *J. Phys. Chem. B* **1998**, *102*, 4061–4063; b) D. C. Magri, R. L. Donkers, M. S. Workentin, *J. Photochem. Photobiol. A* **2001**, *138*, 29–34.
- [10] a) M. S. Workentin, R. L. Donkers, *J. Am. Chem. Soc.* **1998**, *120*, 2664–2665; b) R. L. Donkers, M. S. Workentin, *Chem. Eur. J.* **2001**, *7*, 4012–4020.
- [11] a) S. Antonello, F. Maran, *J. Am. Chem. Soc.* **1997**, *119*, 12595–12600; b) S. Antonello, F. Maran, *J. Am. Chem. Soc.* **1999**, *121*, 9668–9676; c) S. Antonello, F. Formaggio, A. Moretto, C. Toniolo, F. Maran, *J. Am. Chem. Soc.* **2001**, *123*, 9577–9584.
- [12] J.-M. Savéant, *Adv. Phys. Org. Chem.* **2000**, *35*, 117–192.
- [13] a) R. L. Donkers, M. S. Workentin, *J. Am. Chem. Soc.* **2004**, *126*, 1688–1698; b) D. L. B. Stringle, R. N. Campbell, M. S. Workentin, *Chem. Commun.* **2003**, 1246–1247.
- [14] a) A. J. Bard, L. R. Faulkner, *Electrochemical Methods, Fundamentals and applications*, Wiley, New York, 2nd., **2001**. b) The background subtracted voltammograms are transformed to sigmoidal-shaped *i*-*E* curves by use of the convolution integral and the experimental current  $i: I(t) = \frac{1}{\pi^{1/2}} \int_0^t \frac{i(u)}{(t-u)^{1/2}} du$
- [15] J. C. Imbeaux, J.-M. Savéant, *J. Electroanal. Chem.* **1973**, *44*, 169–187.
- [16] a) R. L. Donkers, F. Maran, D. D. M. Wayner, M. S. Workentin, *J. Am. Chem. Soc.* **1999**, *121*, 7239–7248; b) D. C. Magri, M. S. Workentin, *Org. Biomol. Chem.* **2003**, *1*, 3418–3429.
- [17] C. Lacaze-Dufaure, F. Najjar, C. André-Barrès, unpublished results.
- [18] S. Tonmunphean, S. Irlé, S. Kokpol, V. Parasuk, P. Wolschann, *Mol. J. Struct. (Theochem)* **1998**, *454*, 87–90.

Received: March 31, 2006

Published online: October 25, 2006